



EVALUATION OF AN AIR QUALITY SIMULATION OF THE LOWER FRASER VALLEY—II. PHOTOCHEMISTRY

MARK HEDLEY, R. MCLAREN, WEIMIN JIANG and D. L. SINGLETON

Institute for Chemical Process and Environmental Technology, National Research Council of Canada, Ottawa, Canada K1A 0R6

Abstract—The photochemical component of an advanced modelling system for use in pollution control studies is evaluated. Results of a case study for July 1985 in the Lower Fraser Valley region of British Columbia are used to test the performance of the modelling system during an ozone episode. Time series of surface trace pollutant concentrations are used to validate the model prediction. A quantitative analysis of the model errors shows that the modelling system adequately predicts the photochemistry without arbitrary adjustments to the emissions inventory. Improved performance of the ozone forecast would likely be obtained, however, if the non-methane organic compound emissions were increased in urban areas. The mechanistic parameters were shown to be very sensitive to the emissions profile, although the net impact of the parameter changes on ozone production was minor in this case. © 1997 Published by Elsevier Science Ltd. All rights reserved.

Key word index: Ozone, mesoscale modelling, air pollution.

1. INTRODUCTION

One of the most important functions of a photochemical modelling system is to assess the potential effectiveness of pollutant emissions control strategies. The implementation of a control strategy is enormously expensive, and it is imperative that the achievement of the air quality objectives is virtually guaranteed. The nonlinear relationship between emitted chemicals and ambient pollutant concentrations makes it impossible to predict the net effect of regulatory actions on air quality without numerical air quality models (National Research Council, 1991), and therefore the need for accurate and reliable photochemical modelling systems is obvious.

Validation of the modelling system is performed by comparing the results of a forecast against field measurements. This exercise must be done for any region that the model is applied to, since there can be local effects that stress the model assumptions beyond its design parameters. In this study, the validation of a comprehensive photochemical modelling system, MC2-CALGRID, is presented for the Lower Fraser Valley region of Canada.

The Lower Fraser Valley is one of the three areas in Canada that the NO_x-VOC Management Plan of the Canadian Council of Ministers of the Environment (CCME) has identified as having a significant ground-level ozone problem (CCME, 1990). For the three years from the period 1983–1989 with the highest ozone maxima, there were on average 10.7 days per

year where measured ozone mixing ratios exceeded the Canadian air quality objective of 82 ppb for 1 h or more. Therefore, the Lower Fraser Valley has been targeted as an area to implement emissions controls, and this modelling study is intended to supplement the understanding of how potential emissions controls will impact ground-level ozone.

The Lower Fraser Valley provides a unique opportunity to evaluate a photochemical modelling system. The valley itself is characterized by very steep side walls that bound the valley to the north and southeast (Fig. 1). These walls tend to confine and channel air flow off the Strait of Georgia up the valley. Vancouver is a major metropolitan centre that is the source of most of the anthropogenic emissions, and is located at the mouth of the valley. Outside of the urban and suburban portion of the valley, the area is predominantly coniferous forest, and hence there are significant emissions of biogenic non-methane organic compounds (NMOCs) in the summer months.

Although the meteorology of the Lower Fraser Valley is complex and difficult to model, the Lower Fraser Valley remains an attractive region to study because the air quality is determined almost entirely by local emissions. Therefore, the exceedingly difficult task of determining the contribution of trans-boundary pollutants to the local air quality is largely removed. This allows us to model the net effect of emissions control strategies and to assert with confidence that, provided the modelling system behaves well, the modelled response of the atmospheric air

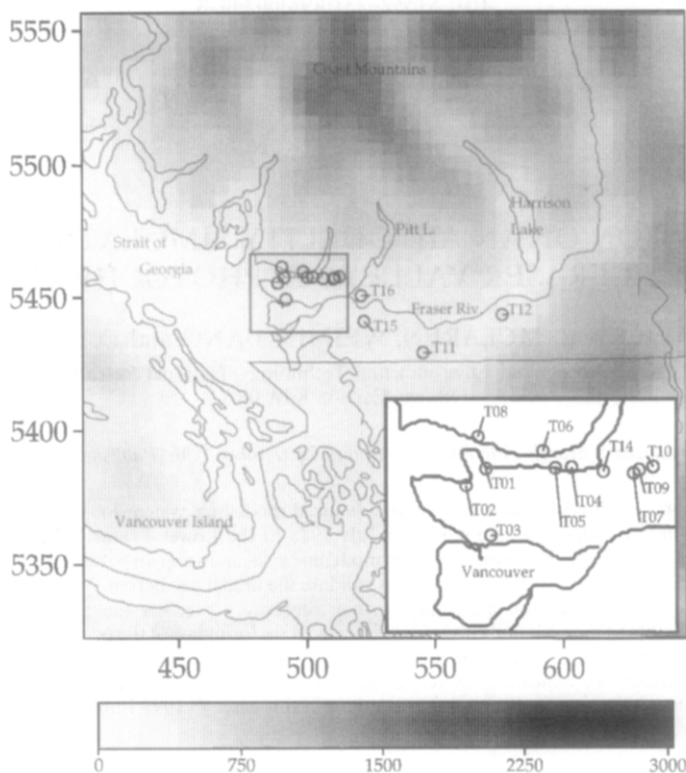


Fig. 1. Map of the Lower Fraser Valley and surrounding area. The shading corresponds to the height of the topography (m) according to the gray scale shown. The open circles show the location of the air quality monitoring stations. The inset provides an expanded view of the Vancouver area. The top of the map is North. The Canada-U.S. border is shown as the thin line running just south of T11 (Abbotsford). The scales along the axes show the UTM coordinates in km.

quality will be similar to the response that would occur in the real atmosphere.

The test case chosen for this paper is a five day period in July 1985, during which the Lower Fraser Valley experienced an ozone episode. The large-scale meteorological situation, described by Hedley and Singleton (1997), was typical of the conditions present during the more severe ozone episodes in the Lower Fraser Valley. The combination of thermally and topographically forced flows during this period provides a rigorous test of the capability of the modelling system.

The range of applicability as well as ultimate performance of a model is limited by the underlying assumptions made in its formulation. For example, if the meteorological component of the system used the hydrostatic assumption, then it would not be useful in a region with steep topography. Similarly, a model with a highly simplified photochemical reaction mechanism could not cope with emissions control strategies that involved large deviations from the average case. Ideally, the photochemical modelling system would contain as few assumptions as possible, and would be flexible enough to adapt to practically any region. This paper introduces the MC2-CALGRID modelling system, which has these desirable features.

For the meteorological component of the modelling system, a state of the art mesoscale forecast model, MC2 (Tanguay *et al.*, 1990, 1992), is used in combination with the CALMET meteorological preprocessor. The results of the meteorological simulation used in the present photochemical simulations for the 17–21 July 1985 ozone episode are discussed at length by Hedley and Singleton (1996).

The photochemical model used in this system is CALGRID, described by Yamartino *et al.* (1992). The CALGRID model is designed to simulate the air quality of urban atmospheres, and has been employed for several pollution studies (Pilinis *et al.*, 1993; Kumar *et al.*, 1994). The model incorporates advanced techniques for the calculation of transport, deposition, and chemical transformation, and has the highly beneficial feature of a completely flexible reaction mechanism. In this study, the reaction mechanism is based on a condensed version of the SAPRC90 scheme (Carter, 1990), and is named COND2243. There are 129 reactions among 54 organic and inorganic species. Details of this mechanism can be found in Jiang *et al.* (1996a).

In addition to the two core models forming MC2-CALGRID, a large package of software is required to model the chemical emissions from the multitude of sources in the Lower Fraser Valley. The emissions are

broadly grouped into anthropogenic and biogenic sources. Anthropogenic emissions are processed using the Emissions Preprocessing System version 2.0 (EPS2) (Gardner *et al.*, 1992). The application of EPS2 to the Lower Fraser Valley to generate the gridded, temporally allocated anthropogenic emissions data was described in detail by McLaren *et al.* (1996). The biogenic emissions are modelled using a modified version of PC-BEIS (Pierce and Waldruff, 1991), where the emissions of volatile organic compounds from vegetation are calculated as functions of the incoming solar radiation and the meteorological forecast from MC2.

2. THE 17–21 JULY 1985 LOWER FRASER VALLEY OZONE EPISODE

The Greater Vancouver Regional District (GVRD) and British Columbia Ministry of the Environment (BCMoE) operate several trace pollutant monitoring sites throughout the Lower Fraser Valley. During the summer of 1985, measurements of O₃, NO₂, NO, CO and SO₂ were made at the station locations indicated in Fig. 1. Unfortunately, there were no upper-level measurements of these species taken during this period. In addition, there were no NMOC measurements at all during this period.

The air quality during the month of July 1985 was quite poor in general, due to the stagnant air conditions caused by the presence of a high-pressure system to the southwest of the Lower Fraser Valley (Hedley and Singleton, 1997). Evidence of the stagnation of the lower troposphere during 17–21 July is clearly shown in the month long time series of CO measurements taken at the urban station T02 for July 1985 (Fig. 2; see Fig. 1 for the station locations). Carbon monoxide is relatively unreactive, and local concentrations are mainly affected by local emissions, advection and diffusion. On many days during the month, very large spikes in CO mixing ratio are observed, with peak values occurring near midnight. The cause of these

peaks is most likely due to the formation of nighttime surface inversions, where even weak emissions of CO can lead to large ambient concentrations. On midnight of 17 July, the observed value of CO was almost 8 ppm.

The time series of hourly ozone mixing ratio for the entire month at station T15 is shown in Fig. 3a. On six days (2, 7, 8, 18–20 July) the ozone mixing ratio exceeded the 1 h Canadian air quality objective of 82 ppb, and on three of those days, the ozone mixing ratio exceeded 100 ppb. The peak mixing ratio measured within the Lower Fraser Valley for the whole month of July was 110 ppb, and was measured at T15 on 20 July.

Station T11 is farther into the rural portion of the Lower Fraser Valley than T15, but the time series of ozone has the same qualitative features (Fig. 3b). The ozone levels at T11 tend to be less than those at T15, especially at night. The high ozone days appear to cluster together into multi-day episodes which are similar between the two time series plots. The ozone exceedances observed during the first ten days of the month at T15 are not apparent at T11. The two episodes occurring in the last half of the month from 17–21 July to 26–29 July are clearly visible in both time series.

The ozone measurements taken at an urban site T02 are shown in Fig. 3c. Compared to the sites outside of the urban core, the ozone levels are very much lower at T02. This is expected, since the urban core is characterized by high concentrations of freshly emitted NO, which reacts quickly with any ambient ozone. At this station, there is only one day that experiences an exceedance, when on 20 July the mixing ratio just barely reached 82 ppb. It is notable that this happened to be a Saturday, when one would expect that anthropogenic emissions of ozone precursors are significantly lower than on a weekday.

At the Robson Square station (T01), the ozone mixing ratios are lower yet (Fig. 3d), with the one exception of 20 July, where the same ozone spike is seen as at T02. It appears that this urban ozone spike is a robust feature in the observations. The rural sites

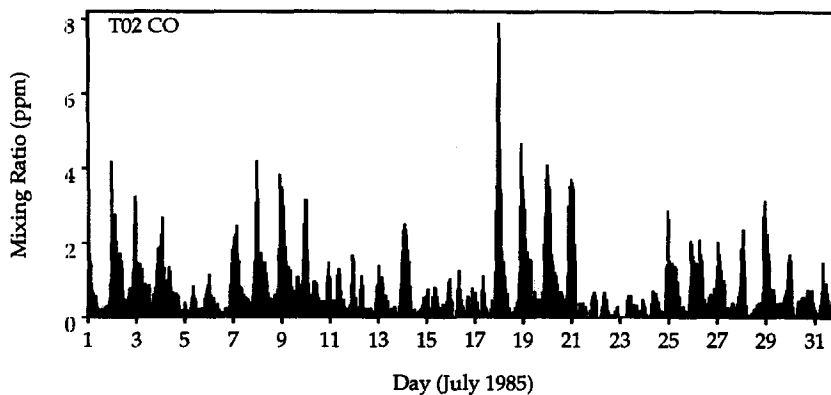


Fig. 2. Time series of carbon monoxide mixing ratios for July 1985 at station T02.

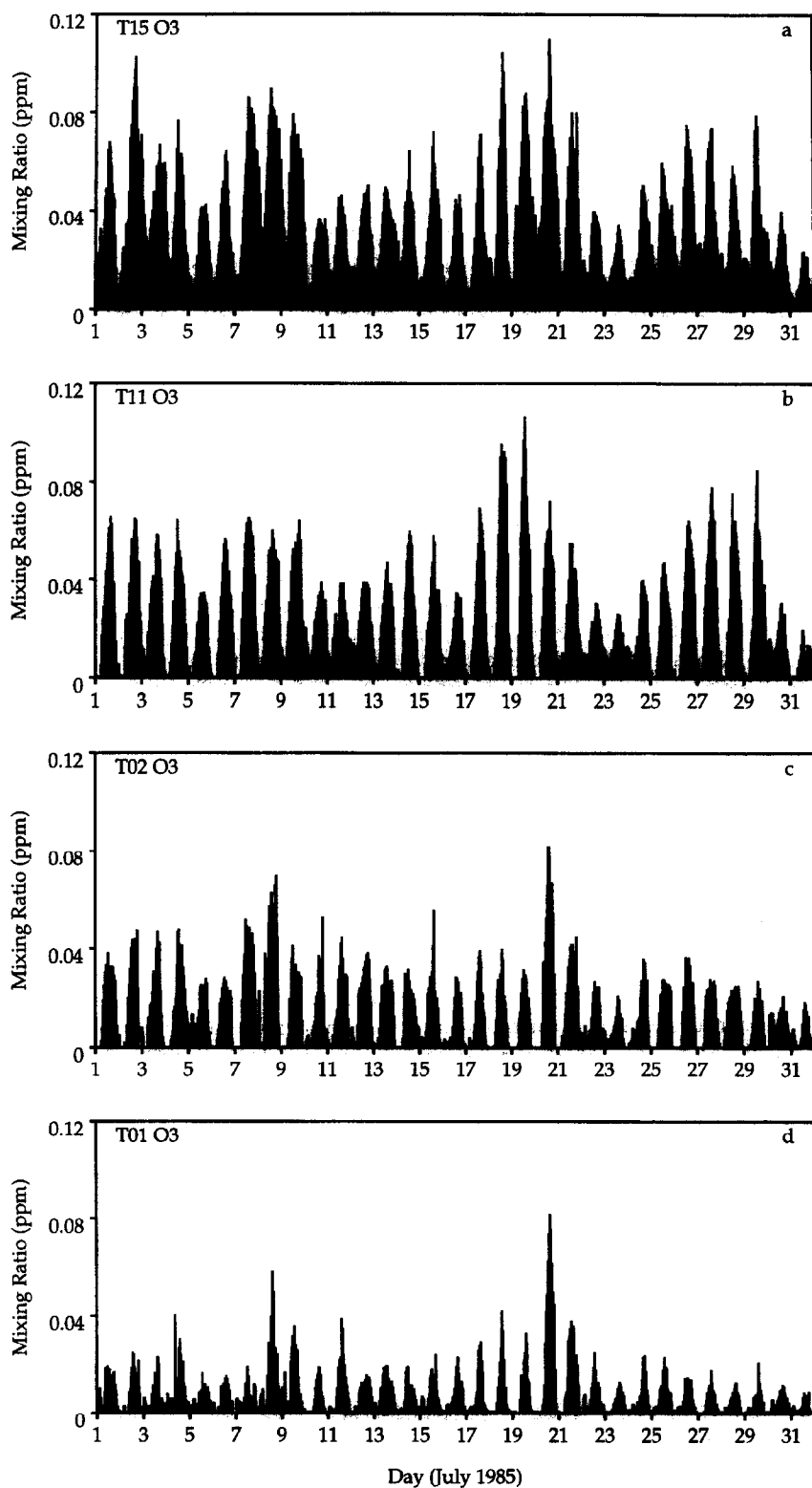


Fig. 3. Time series of ozone mixing ratios for July 1985 at station (a) T15, (b) T11, (c) T02, and (d) T01.

do not exhibit this particular phenomenon, and in fact the rural sites show that the episode is rapidly decaying on 20 July. This feature will be commented on in more depth in a later section.

It is interesting that during the observed ozone episodes, the night time surges of CO that were noted at T02 are even more significant than usual. This is evidence that the conditions for the development of an

ozone episode are closely related to the state of the lower atmosphere.

The rest of the paper will focus on the 17–21 July ozone episode.

3. MODEL EVALUATION

The horizontal domain for CALGRID is the same as that shown in Fig. 1. It is a 240 km × 240 km square on a Universal Transverse Mercator (UTM) projection. The horizontal resolution used for this domain is 5 km, which was chosen to match the resolution of the emissions database. The depth of the photochemical grid is set to 5 km and is divided into 10 levels of varying depth (Table 1).

Table 1. Heights of the layer faces for the photochemical simulation

Level	Z _f (m)	Level	Z _f (m)
11	5000	5	260
10	3600	4	160
9	2200	3	80
8	1200	2	20
7	660	1	0
6	410		

The meteorological simulation was carried out using MC2 on a larger domain, and then processed using CALMET to produce the meteorological data set that CALGRID requires on the above grid. A full description of the performance of the MC2-CALMET model combination was given by Hedley and Singleton (1997).

For the photochemical simulation, the initial mixing ratios of the trace pollutants were set to values typical for a clean rural atmosphere as follows: O₃ = 15 ppb (parts per billion), NO_x = 2 ppb, NMOC = 17 ppbC (ppb of carbon) and CO = 200 ppb. The decision to begin with such clean initial conditions was based on the belief that the emissions themselves would eventually drive the simulation towards realistic pollutant concentrations.

The processing of the episode-specific emissions data used in the following simulations were described in detail by McLaren *et al.* (1996). The anthropogenic emissions of NO for 0800 PST on 17 July are shown in Fig. 4. The large rush hour emissions clearly show the location of the urban core of Vancouver.

The simulation was initiated at 0400 PST, 17 July and run for 116 h until 0000 PST 22 July. All calculations were performed on a Silicon Graphics Power Indigo2 desk top workstation with 64 Mbytes of memory. The CPU requirements for the MC2

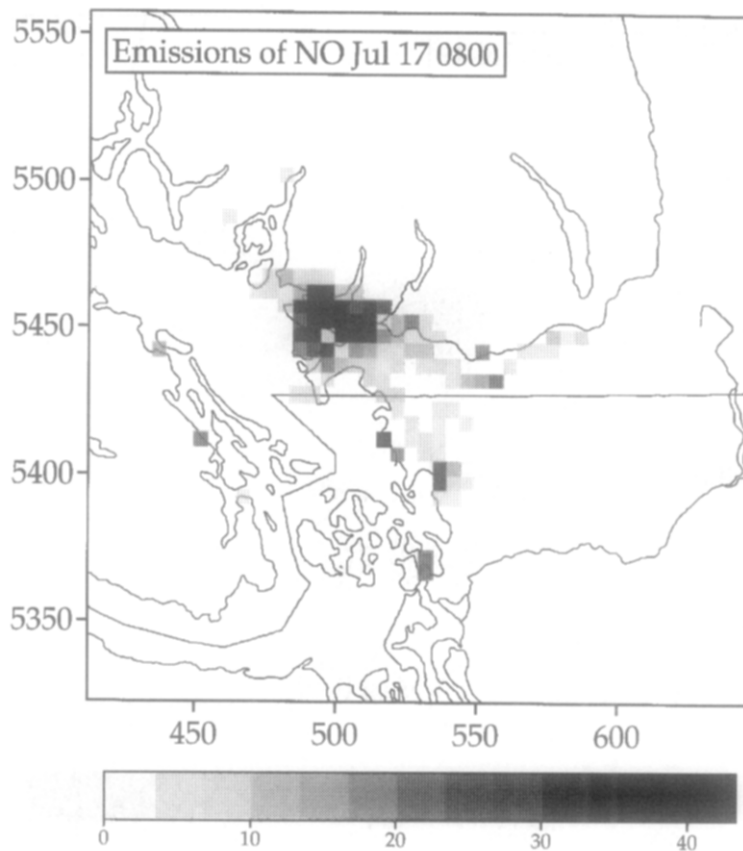


Fig. 4. Anthropogenic NO emissions for 0800 PST on 17 July. The shading indicates the magnitude of the emissions in terms of g s^{-1} per grid cell according to the gray scale shown.

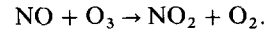
simulation were 40 min of CPU time for every hour of simulated time. The CALGRID simulation required 1.5 h of CPU time for every 24 h of simulation.

3.1. Surface fields

The simulated surface mixing ratio field for NO_x on 19 July at 1500 PST is shown in Fig. 5. The peak values occur over the urban core of the city of Vancouver. A plume of NO_x extends downwind from the urban core, extending along the Lower Fraser Valley. Note the locations of the secondary maxima along the Washington coastline and on Vancouver Island, which are caused by large industrial point source emissions.

The surface CO mixing ratio for 19 July at 1500 PST (Fig. 6) shows how the urban plume extends into the Lower Fraser Valley more clearly than NO_x , due to its longer chemical lifetime. The ozone field for this time (Fig. 7) reveals that the model predicted over 100 ppb in some areas. The peak value of 106 ppb occurred on the American side of the border south of Chilliwack. Just to the west of Harrison Lake, there were also a few grid points with greater than 100 ppb. Another local maximum is located near Abbotsford, with values greater than 80 ppb. Directly over the urban core of Vancouver, it is seen that there is a local

minimum of ozone. This is due to the titration of ozone by the local sources of NO emitted from automobiles, via the reaction



3.2. Statistical evaluation

A quantitative assessment of the accuracy of the base case model prediction can be made using the statistical measures suggested by Willmott (1981, 1982) and Willmott *et al.* (1985), as Steyn and McKendry (1988) did in evaluating their meteorological simulation of the Lower Fraser Valley. We use the same terminology and definitions as presented in those papers and in Hedley and Singleton (1997), including the observed and modelled means and standard deviations of the data; the slope, b , and the intercept, a , of the least-squares linear regression of predicted vs observed data; the root-mean-squared difference, E , between the modelled data (P_i) and observed data (O_i); and the index of agreement, d , calculated as

$$d = 1 - \frac{E^2}{\langle (|P_i| + |O_i|)^2 \rangle}$$

where the primed quantities are the departures from the mean observed value, and the angle brackets

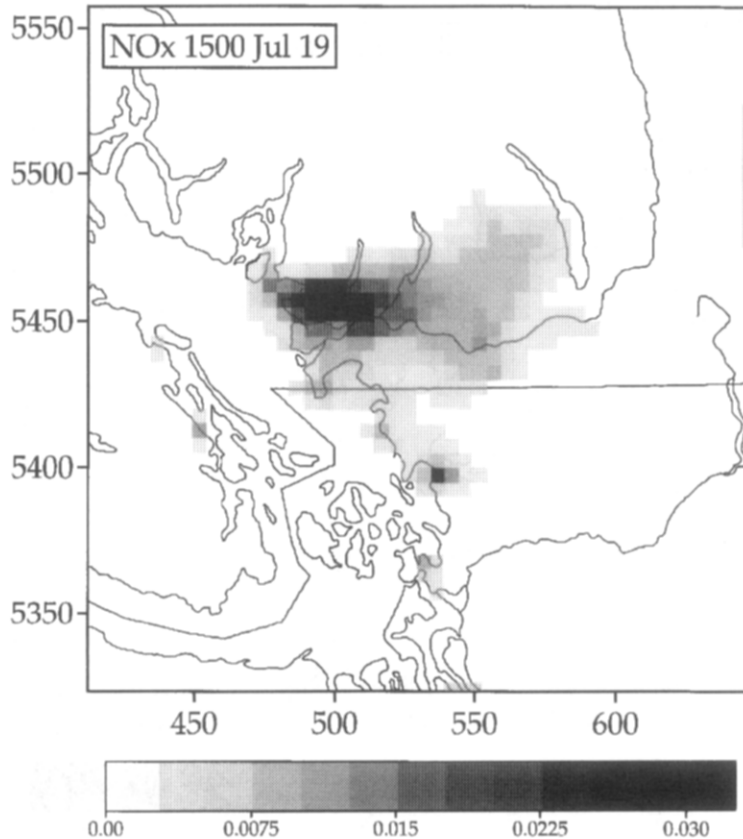


Fig. 5. Simulated surface mixing ratio fields at 1500 PST, 19 July for NO_x . The gray scales show the mixing ratios in parts per million (ppm).

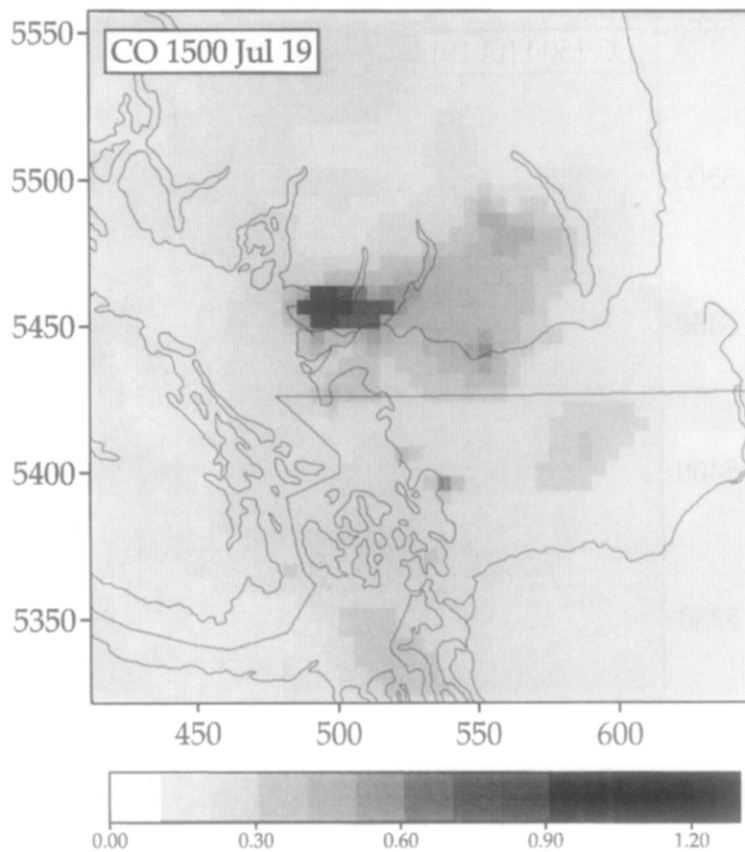


Fig. 6. Simulated surface mixing ratio of carbon monoxide at 1500 PST, 19 July. The gray scales show the mixing ratios in parts per million (ppm).

denote the averaging operator. A value of $d = 1$ indicates perfect agreement, and $d = 0$ indicates absolutely no agreement.

There are many other measures that have been used to evaluate photochemical model performance. In Jiang *et al.* (1996b), we used a slightly modified version of the measures suggested by Tesche (1988) to compare the performance of MC2-CALGRID against the SAIMM/UAM-V modelling system in simulating the first four days of the ozone episode discussed in this paper.

As recommended by Willmott (1981), E is further decomposed into two parts, E_S and E_U , which represent the systematic and unsystematic portions of E , respectively. The systematic component is the RMS difference between the observed data and the least-squares linear regression of the predicted vs observed data, $P_i^* = a + bO_i$, while the unsystematic component is the rms difference between the predicted data and P_i^* . The systematic component is caused entirely by non-zero values of the linear regression intercept (a), and values of the slope (b) unequal to one. The unsystematic component is due to any nonlinear variation of the predicted values against observations. The relation $E^2 = E_S^2 + E_U^2$ was shown by Willmott (1981). Interpretations of the above parameters are provided by Willmott (1981, 1982) and Willmott *et al.*

(1985), and summarized by Hedley and Singleton (1997).

In this study, as in Hedley and Singleton (1997), the averages calculated in the above definitions are averages over time, and the statistics are calculated for each observing station. By calculating the performance statistics for each station, systematic errors in the forecast caused by local effects are clearly highlighted, as will be shown below.

The NO_x time series for T04 (Fig. 8a) reveals that the model accurately predicts daytime NO_x levels for the first 3 days of the simulation. The plot of predicted vs observed NO_x (Fig. 8b) shows a fairly good linear agreement with a slope of 0.49 and intercept of 14 ppb. It should be noted that only daytime measurements are included in the observed NO_x data since the observed extremely high nighttime values proved almost impossible to simulate. Although there were no nighttime measurements of mixed layer depths taken, it is reasonable to assume that the observed high nighttime values of NO_x were due to emissions into a shallow nocturnal surface inversion. Hedley and Singleton (1997) showed that the meteorological simulation had difficulty in predicting temperatures and mixed layer depths at overland sites within a small number of grid points of the shoreline, due to an overestimation of the moderating effect of water

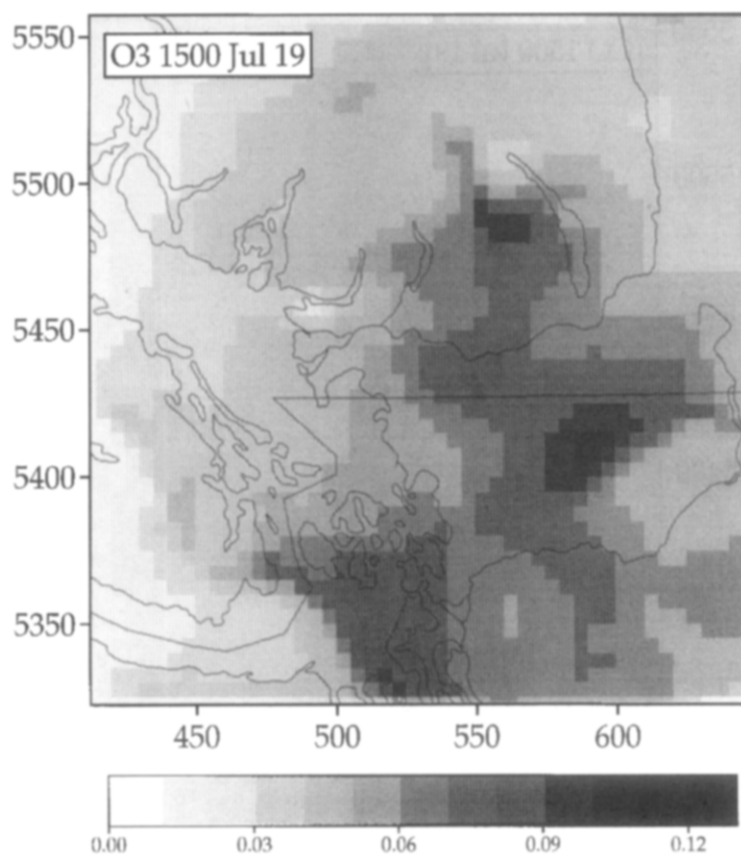


Fig. 7. Simulated surface mixing ratio fields at 1500 PST, 19 July for ozone. The gray scales show the mixing ratios in parts per million (ppm).

temperatures on air temperatures. Slight errors in the mixing parameters near the surface can lead to large errors in the forecast nighttime boundary layer, and therefore large errors in the forecast concentrations.

The NO_x performance results are shown in Table 2 for all the other stations. With the exception of T15 and T16, the indices of agreement for NO_x are all above 0.5, with a maximum value of 0.83 at T05. The predicted observed averages are acceptably close for all stations, except possibly for T15 and T16. In general, the model tends to underpredict the standard deviations, although for the urban sites T02 and T03 the standard deviations were overestimated. Total RMS errors were less than 20 ppb at all sites except T15. It should be noted that no attempt was made to adjust the observed NO_x data to correct for possible interference from the presence of nitrates, which can cause overestimation of observed NO_x by about 10%.

The measured and predicted CO time series for T04 is shown in Fig. 8c. As with the NO_x data, it should be noted that only daytime measurements are included in the observed data. In general, the model performs well at capturing the day-to-day variation in overall CO concentration. The model tends to overestimate CO at rush hours, and it appears that the rush hour

cycle is more pronounced in the model results than in the observed data.

The plot of predicted vs observed CO at T04 (Fig. 8d) follows a reasonably linear relationship, although the least-squares slope is rather low and the intercept is high (Table 3). The relatively small value for E_U is quantitative evidence that the linear relationship is robust. The index of agreement for this station of 0.67 is encouragingly high.

The performance statistics for the other CO measuring stations are also listed in Table 3. The two stations closest to the urban core, T08 and T02, have the lowest indices of agreement. The poor performance of the model in the downtown core is likely due to errors in the boundary-layer depth and other surface mixing parameters resulting from the proximity of the urban stations to the coast. The large emissions arising from the urban core into the boundary layer make the model very sensitive to any errors in the boundary-layer calculations. At T03, which is just south of the urban core, the performance is better, and farther inland at T10 the results are still better.

It is clear that the distribution of NO_x and CO monitoring sites is too closely grouped around the urban core. This makes hourly measurements too sensitive to local emissions rates and therefore difficult

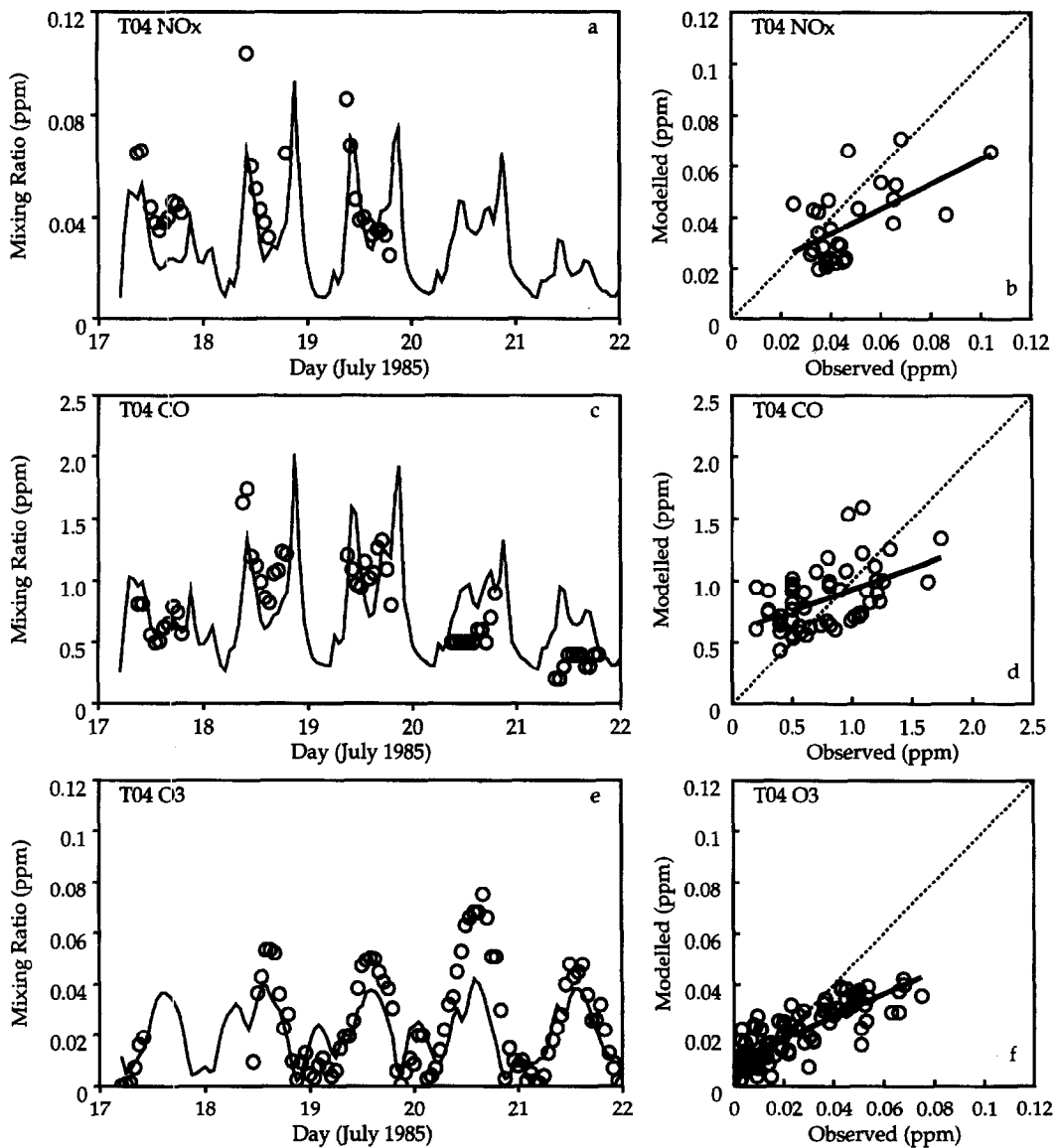


Fig. 8. Station T04 time series and scatter plots of predicted and observed mixing ratios. Time series: (a) NO_x , (c) CO, and (e) ozone. Observed values are plotted as circles. Scatter plots of (b) NO_x , (d) CO, and (f) ozone. The least-squares linear regressions are indicated by the thick lines. The dashed lines have slopes of unity and intercepts of zero, representing perfect forecasts.

Table 2. NO_x time-series statistics^a

Station	n	$\langle c_o \rangle$	$\langle c_p \rangle$	δ_o	δ_p	b	a	E	E_s	E_U	d
T02	27	34.6	43.5	7.5	20.0	1.72	-15.9	18.3	10.3	15.1	0.55
T03	33	19.5	25.4	12.7	13.5	0.62	13.4	13.3	7.6	10.9	0.73
T04	28	47.5	37.3	17.7	14.8	0.49	14.0	17.9	13.5	11.8	0.67
T05	33	55.1	55.4	27.2	17.1	0.49	28.5	17.3	13.7	10.6	0.83
T07	33	24.3	28.4	10.4	9.5	0.42	18.1	11.0	7.2	8.3	0.66
T10	33	32.1	25.0	11.1	8.8	0.34	14.2	12.9	10.1	7.9	0.58
T14	33	32.6	30.9	14.0	10.9	0.47	15.6	11.4	7.5	8.6	0.76
T15	32	27.4	11.5	12.0	5.5	-0.04	12.5	20.8	20.1	5.3	0.44
T16	23	29.9	19.5	13.7	6.6	0.04	18.3	17.8	16.6	6.4	0.47

^a The terms n , b and d are dimensionless. All other terms have dimension ppb. The o and p subscripts refer to observed and predicted values, respectively. The standard deviations are represented by δ . The time-averaged species mixing ratios are denoted by $\langle c \rangle$.

Table 3. Carbon monoxide time-series statistics^a

Station	<i>n</i>	$\langle c_o \rangle$	$\langle c_p \rangle$	δ_o	δ_p	<i>b</i>	<i>a</i>	<i>E</i>	<i>E_s</i>	<i>E_U</i>	<i>d</i>
T02	55	359	1145	212	568	1.37	652	925	789	483	0.32
T03	33	1008	629	198	229	0.07	559	477	421	225	0.40
T04	54	767	849	361	247	0.35	584	326	248	211	0.67
T08	55	524	1003	312	955	1.29	327	987	488	858	0.37
T10	33	488	660	225	203	0.26	532	305	237	191	0.46

^a The terms *n*, *b* and *d* are dimensionless. All other terms have dimension ppb. The o and p subscripts refer to observed and predicted values, respectively. The standard deviations are represented by δ . The time-averaged species mixing ratios are denoted by $\langle c \rangle$.

Table 4. Ozone time series statistics^a

Station	<i>n</i>	$\langle c_o \rangle$	$\langle c_p \rangle$	δ_o	δ_p	<i>b</i>	<i>a</i>	<i>E</i>	<i>E_s</i>	<i>E_U</i>	<i>d</i>
T01	109	14.3	11.6	18.3	8.8	0.34	6.8	13.9	12.4	6.3	0.70
T02	114	17.4	14.2	19.8	11.4	0.47	6.1	12.8	10.9	6.6	0.82
T03	67	14.5	17.6	16.0	14.7	0.85	5.2	6.6	3.8	5.4	0.95
T04	92	24.8	20.9	20.3	11.0	0.44	9.9	13.5	11.9	6.3	0.80
T05	115	27.5	17.9	23.4	10.6	0.35	8.1	19.0	17.9	6.6	0.70
T06	59	19.2	17.8	17.7	10.4	0.42	9.8	12.6	10.4	7.2	0.78
T07	116	38.4	26.4	25.1	13.2	0.39	11.3	21.3	19.4	8.7	0.70
T09	116	32.6	27.0	30.5	13.0	0.30	17.1	23.7	21.9	9.1	0.68
T10	48	33.7	30.0	24.5	12.7	0.25	21.5	21.5	18.4	11.0	0.60
T11	116	32.0	45.3	29.8	16.7	0.43	31.5	24.1	21.5	10.8	0.76
T12	114	35.5	46.9	32.0	13.4	0.30	36.1	26.6	24.9	9.2	0.69
T13	55	28.1	23.0	12.8	12.0	0.66	4.6	10.9	6.7	8.6	0.79
T15	115	44.5	34.3	27.7	16.8	0.43	15.2	22.2	18.8	11.8	0.74
T16	93	31.3	31.0	30.1	16.3	0.40	18.5	20.9	17.9	10.8	0.78

^a The terms *n*, *b* and *d* are dimensionless. All other terms have dimension ppb. The o and p subscripts refer to observed and predicted values, respectively. The standard deviations are represented by δ . The time-averaged species mixing ratios are denoted by $\langle c \rangle$.

to compare against model predictions. It would be highly beneficial to have more monitoring sites located farther inland and away from major highways and industrial facilities.

The ozone time series for T04 (Fig. 8e) shows that with the exception of the second to last day, the model predicts ozone mixing ratios well. (Note that for the ozone time series, nighttime observations are included in the graphs and the subsequent analysis.) The peak values are underestimated by about 10 ppb each day except Saturday, 20 July, when the peak mixing ratio was underestimated by over 33 ppb. The model predicted nighttime increases in ozone that were somewhat high, although the results for the early morning of 20 July are very good.

The predicted ozone at T04 shows a good linear relationship with the observed values, although the model shows a tendency to underforecast the peaks and overforecast the minimum values (Fig. 8f). The points are tightly grouped about the *P** line, with an unsystematic RMS error component of only 6 ppb (Table 4). The modelled average mixing ratio was off by -4 ppb, and the predicted standard deviation was about half of the observed 20 ppb. The overall performance of the simulation at this station was very acceptable with an index of agreement of 0.81.

The occurrence of a large ozone surge on a Saturday is curious, and was measured at several sites in the downtown and surrounding area (see Fig. 3d for the T01 time series). It was not reported in the rural areas, such as T11 (Fig. 3d). It is possible that it was caused by left over precursors and ozone from the Friday which were subsequently mixed down to the surface on Saturday afternoon, an event not captured by the model. The absence of any significant morning rush hour on Saturday would lead to reduced destruction of ozone, and thus higher observed ozone concentrations. The failure of the model to predict this effect may be an indication the modelled nighttime drainage flow was too efficient at cleaning the Lower Fraser Valley of ozone and its precursors on the Friday night.

The performance statistics for ozone predictions at all stations are listed in Table 4. The model performs extremely well for most stations, with indices of agreement ranging from 0.60 to 0.95. The high precision of the model is indicated by the small values of *E_U*, which are less than or equal to 12 ppb for all stations; in other words, the model results vary almost linearly with the observations.

The relatively large values of the linear regression intercept, *a*, for the rural stations T11 and T12 indicate

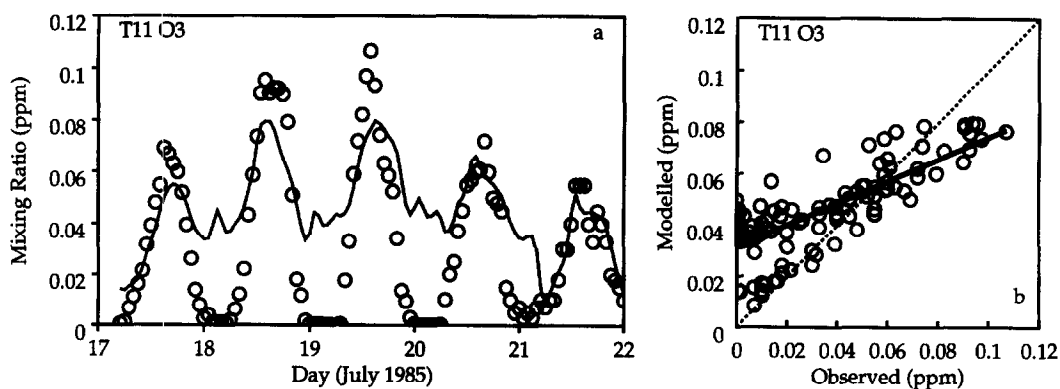


Fig. 9. (a) Ozone mixing ratio (ppm) time series for station T11. Observed values are plotted as circles. (b) Scatter plot of predicted vs observed ozone mixing ratios. The least-squares linear regression is indicated by the thick line, and the perfect forecast is represented by the dashed line.

that although the model is excellent at predicting the ozone peaks and day-to-day variation of ozone in the rural areas, the model has some difficulty in producing the low nighttime concentrations of ozone measured at these sites. This is readily apparent in the ozone time series and scatter plot for T11 (Figs 9a and b). The causes of the nighttime overestimates could be a combination of the following problems:

- The predicted nighttime inversion at the surface may not be developed adequately enough. If there is too much vertical mixing at the surface, then ozone could continuously mix down to replace the ozone that is removed by deposition. In addition, too much mixing would dilute the ozone-destroying effect of any nighttime NO emissions.
- The local emissions of NO may be underestimated in the rural areas during the night.
- The rate of surface deposition of ozone may be underestimated.

Further sensitivity tests are being carried out to determine the likely cause of the overestimates.

3.3. Sensitivity of ozone to kinetic parameters

To show the effect of using a default emissions profile to determine the kinetic parameters for the chemical mechanism rather than calculating the parameters based on the local emissions profile, an experiment was run using the parameters that are shipped with CALGRID. These parameters are listed in the file named CG082787.RXP, and were based on data from the Southern California Air Quality Study (SCAQ) (Lawson, 1990). Some of the major differences between the mechanistic parameters are described below.

The molecular weight of the most reactive olefin class (OLE3) based on the SCAQS data was 89.62 g mol^{-1} . This is a substantial decrease compared to the value of $116.43 \text{ g mol}^{-1}$ that resulted when the Lower Fraser Valley emissions data was

used. In addition, the carbon number of OLE3 decreased from 8.55 to 6.58 carbons per molecule. These differences result from the greater proportion of NMOC emissions arising from the large biogenic emissions in the Lower Fraser Valley compared to the SCAQS region.

The reaction rates of various organic reactions also changed significantly. The reaction of the hydroxyl radical ($\text{OH}\cdot$) with OLE3 increased from 1.05×10^4 to $1.55 \times 10^4 \text{ ppm}^{-1} \text{ min}^{-1}$ from the Lower Fraser Valley case to the default case. The smaller value in the Lower Fraser Valley case was caused by the increased proportion of the less-reactive biogenic terpenes relative to the highly reactive isoprene within the OLE3 species category, due to the predominantly coniferous forests surrounding the Lower Fraser Valley. For the reaction of $\text{OH}\cdot$ with the alkane class ALK2, the reaction rate decreased from $1.92 \times 10^4 \text{ ppm}^{-1} \text{ min}^{-1}$ in the Lower Fraser Valley case to $1.55 \times 10^4 \text{ ppm}^{-1} \text{ min}^{-1}$ in the default case. In addition, the product yields for many of the organic reactions changed substantially. These are large changes in light of the fact that this is not a control scenario.

The impact of using the default kinetic parameters compared to those calculated specifically for the Lower Fraser Valley are shown in Fig. 10. This plot shows the ozone predicted in the default case minus the ozone predicted in the base case for 1500, 19 July 1985. The differences range from 2.3 to -0.8 ppb. In general, the default kinetic parameters tend to produce slightly higher ozone predictions than the Lower Fraser Valley base case. This is probably due in part to the lower $\text{OH}\cdot$ reactivity of the OLE3 category discussed above, which would lead to diminished peroxy radical production. In terms of ozone production, it is clear that the effects of the large kinetic parameter differences noted above are buffered in this case. However, it is not at all obvious that this would be the case for an emissions control scenario, where the emissions profile could depart radically from the base case.

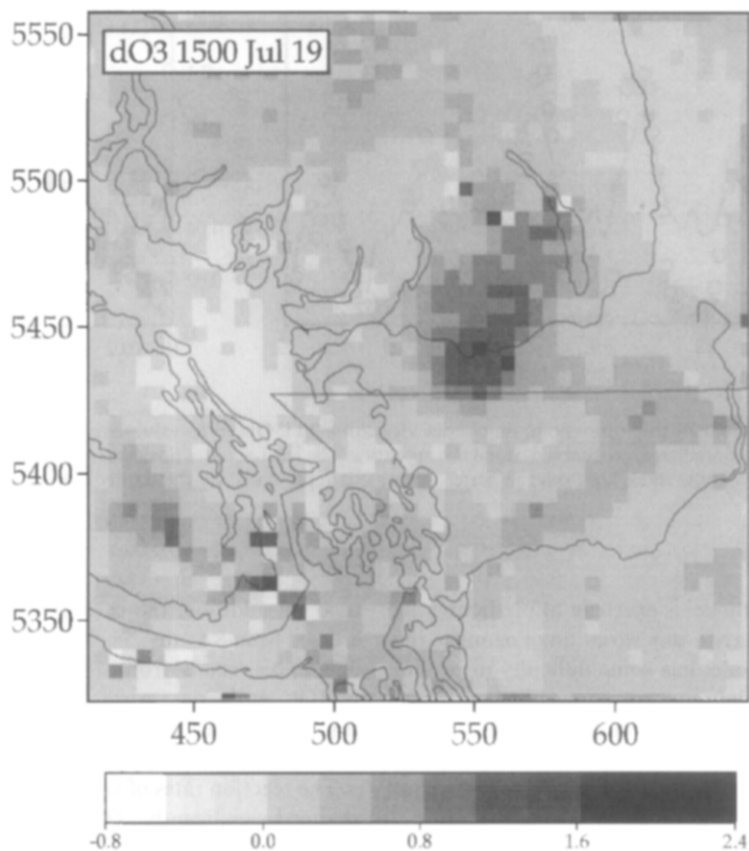


Fig. 10. Surface ozone differences between the experiments run using the default SCAQS-based and the Lower Fraser Valley-based mechanistic parameters for 1500 PST, 19 July. The gray scale shows the differences in mixing ratios in ppb.

4. SUMMARY AND DISCUSSION

The results of the detailed quantitative error analysis show that the MC2-CALGRID photochemical modelling system predicts the photochemical situation with acceptable precision for the five day simulation presented.

Daytime values of the nitrogen oxide and carbon monoxide concentrations were predicted reasonably well at most sites, including the urban core. The model tended to underpredict peak ozone, but in general there was a highly linear relationship between predicted and observed ozone. The model failed to capture the surge of ozone that occurred on the Saturday in the urban core, and the nighttime concentrations at the rural sites was overestimated.

The mechanistic parameters are very sensitive to the organic emissions profile, and a brief comparison of the parameters resulting from the SCAQS emissions profile and the Lower Fraser Valley profile illustrated the large differences that result from relatively small profile changes.

The net impact of these differences on ozone production was shown to be relatively minor in this case, but larger effects could occur in control strategy simu-

lations. Future work will include examination of other groupings of lumped NMOCs that are less sensitive to reasonable changes in emissions profiles.

One of the most significant problems in validating a modelling system in the Lower Fraser Valley is that the distribution of monitoring stations is too dense in the urban core and too sparse everywhere else. It would be highly beneficial to have several stations located farther up the valley, and to have at least one station in the northern part of the Strait of Georgia to measure the pollutant concentrations of the air parcels that eventually enter the valley.

An area that we have not examined in this study is the sensitivity of the model results to the details of the dry deposition mechanism and parameters. The ADOM (Venkatram *et al.*, 1988) style of dry deposition for ozone is employed in CALGRID, and recent work by Padro *et al.* (1992) has identified canopy wetness, among other factors, as having an important influence on deposition velocities.

Recent studies have suggested that deficiencies in model predictions of ozone are due primarily to uncertainties in the NMOC emissions estimates, particularly from motor vehicles and vegetation. For example, Harley *et al.* (1993) simulated the 27–29

August 1987 SCAQS intensive monitoring period, using the CIT photochemical model, and underpredicted ozone levels by about 23% on average. They then used the results of a tunnel study in Los Angeles to justify an increase of organic gas emissions from engine exhaust by a factor of 3, which significantly improved the ozone forecast. Recent work by Geron *et al.* (1994) shows that the biogenic emissions produced by BEIS can be a factor of 5–10 too low when compared against measurements for certain U.S. counties and certain types of vegetation.

Although these studies present evidence that the NMOC emissions can be problematic, there is no comparable evidence that the mobile or biogenic emissions inventories are underestimated in the present study. The recent Cassiar Tunnel study in Vancouver indicated that the mobile emissions model MOBILE5C, the Canadian version of MOBILE5a that was used to develop the mobile emissions for the Canadian portion of the domain, adequately represented light duty vehicle emission factors for the driving conditions in the tunnel (Gertler *et al.*, 1996). Unfortunately, there has not yet been an evaluation of the biogenic emissions model for the land cover type in the Lower Fraser Valley. Our own sensitivity studies with the MC2-CALGRID system show that increased NMOC emissions, especially in the urban regions, would improve the model performance for ozone. However, in the current study, there are no NMOC measurements to compare against (although the NMOC concentrations produced by the model are within the range of variability of observations for later years reported by Dann, 1994), and therefore we have no basis on which to modify the anthropogenic or biogenic emissions estimates.

Although it is clear there is room for improvement, the above results are encouraging. The model adequately captured the general features of the ozone episode without arbitrary adjustments to the emissions inventory. The next stage of this study will be to evaluate a number of emissions control strategies using this simulation as the base case scenario. In addition, the sensitivity of the model to changes in emissions, meteorological grid spacing, deposition parameters and chemical mechanism details will be presented in future papers. Finally, in order to establish further the accuracy of the MC2-CALGRID modelling system, the Pacific 93 episode (Steyn *et al.*, 1996) will be simulated and compared against the rich set of measurements made during that intensive monitoring operation.

Acknowledgements—The authors thank Ms S. Bohme and Mr A. Dorkalam for their work on preparing the emissions data sets for this study. The quality control procedures for the emissions inventory processing implemented by Ms Bohme are especially appreciated. This research was funded by Natural Resources Canada through the Panel on Energy Research and Development and by the National Research Council of Canada.

REFERENCES

- Canadian Council of Ministers of the Environment (1990) *Management Plan for Nitrogen Oxides (NO_x) and Volatile Organic Compounds (VOCs) Phase I*. ISBN 0-191074-70-7.
- Carter, W. (1990) A detailed mechanism for the gas-phase atmospheric reactions of organic compounds. *Atmospheric Environment* **24A**, 481–518.
- Dann, T., Wang, D., Steenkamer, A., Halman, R. and Lister, M. (1994) Volatile organic compound measurements in the Greater Vancouver Regional District (GVRD) 1989–1992. Report No. PMD 94-1, Technology Development Directorate, Environmental Technology Centre, Environment Canada.
- Gardner, L., Causley, M., Wilson, G. and Jimenez, M. (1992) *User's Guide for the Urban Airshed Model Volume IV: User's Manual for the Emissions Preprocessor System 2.0*, SYSAPP-92/059a, Systems Applications International, San Rafael, California.
- Geron, C. D., Guenther, A. B. and Pierce, T. E. (1994) An improved model for estimating emissions of volatile organic compounds from forests in the eastern United States. *J. geophys. Res.* **99**, 12,773–12,791.
- Gertler, A. W., Wittorff, D. N., McLaren, R., Belzer, W. and Dann, T. (1996) Characterization of vehicle emissions in Vancouver BC during the 1993 Lower Fraser Valley Oxidants study. *Atmospheric Environment* (in press).
- Harley, R. A., Russell, A. G., McRae, G. J., Cass, G. R. and Seinfeld, J. H. (1993) Photochemical modeling of the Southern California air quality study. *Envir. Sci. Technol.* **27**, 378–388.
- Hedley, M. A. and Singleton, D. L. (1997) Evaluation of an air quality simulation of the Lower Fraser Valley—Part I. Meteorology. *Atmospheric Environment* **31**, 1605–1615.
- Jiang, W., Singleton, D. L., McLaren, R. and Hedley, M. (1996a) Sensitivity of ozone concentrations to rate constants in a modified SAPRC90 chemical mechanism used for Canadian Lower Fraser Valley ozone studies. *Atmospheric Environment* (in press).
- Jiang, W., Hedley, M. and Singleton, D. L. (1996b) Comparison of the MC2/CALGRID and SAIMM/UAM-V photochemical modelling systems in the Lower Fraser Valley, British Columbia. *Atmospheric Environment* (submitted).
- Kumar, N., Russell, A. G., Tesche, T. W. and McNally, D. E. (1994) Evaluation of CALGRID using two different ozone episodes and comparison to UAM results. *Atmospheric Environment* **28**, 2823–2845.
- Lawson, D. R. (1990) The Southern California air quality study. *J. Air Waste Man. Ass.* **40**, 156–165.
- McLaren, R., Bohme, S., Hedley, M., Jiang, W., Dorkalam, A. and Singleton, D. L. (1996) Emissions inventory processing for UAM-V and CALGRID modelling in the Lower Fraser Valley. *The Emission Inventory: Programs and Progress*, **VIP-56**, 749–755, Air and Waste Management Association, Pittsburgh, Pennsylvania.
- National Research Council (1991) *Rethinking the Ozone Problem in Urban and Regional Air Pollution*. National Academy Press, Washington, DC.
- Padro, J., Neumann, H. H. and Den Hartog, G. (1992) Modelled and observed dry deposition velocity of O₃ above a deciduous forest in the winter. *Atmospheric Environment* **26**, 775–784.
- Pierce, T. E. and Waldruoff, P. S. (1991) PC-BEIS: a personal computer version of the Biogenic Emissions Inventory System. *J. Air Waste Man. Ass.* **41**, 937–941.
- Pilinis, C., Kassomenos, P. and Kallos, G. (1993) Modeling of photochemical pollution in Athens, Greece—application of the Rams-Calgrid modeling system. *Atmospheric Environment* **27B**, 353–370.
- Steyn, D. G. and McKendry, I. G. (1988) Quantitative and qualitative evaluation of a three-dimensional mesoscale

- numerical model simulation of a sea breeze in complex terrain. *Mon. Weath. Rev.* **116**, 1914–1926.
- Steyn, D. G., Bottenheim, J. W. and Thomson, R. B. (1996) Overview of tropospheric ozone in the Lower Fraser Valley, and the PACIFIC '93 field study. *Atmospheric Environment* (submitted).
- Tanguay, M., Robert, A. and Laprise, R. (1990) A semi-implicit semi-Lagrangian fully compressible regional forecast model. *Mon. Weath. Rev.* **118**, 1970–1980.
- Tanguay, M., Yakimiw, E., Ritchie, H. and Robert, A. (1992) Advantages of spatial averaging in semi-implicit semi-Lagrangian schemes. *Mon. Weath. Rev.* **120**, 113–123.
- Tesche, T. W. (1988) Accuracy of ozone air quality models. *J. Envir. Engng* **114**, 739–752.
- Venkatram, A., Karamchandani, P. K. and Misra, P. K. (1988) Testing a comprehensive acid deposition model. *Atmospheric Environment* **22**, 737–747.
- Willmott, C. J. (1981) On the validation of models. *Phys. Geography* **2**, 168–194.
- Willmott, C. J. (1982) Some comments on the evaluation of model performance. *Bull. Am. Met. Soc.* **63**, 1309–1313.
- Willmott, C. J., Ackleston, S. G., Davis, R. E., Feddema, J. J., Klink, K. M., Legates, D. R., O'Donnell, J. and Rowe, C. M. (1985) Statistics for the evaluation and comparison of models. *J. geophys. Res.* **90**, 8995–9005.
- Yamartino, R. J., Scire, J. S., Carmichael, G. R. and Chang, Y. S. (1992) The CALGRID mesoscale photochemical grid model—I. Model formulation. *Atmospheric Environment* **26A**, 1493–1512.